Journal of Nepal Geological Society, 2011, Vol. 43 (Special Issue), pp. 1–12

Geological and structural architecture of the Kangchenjunga region, eastern Nepal

***Pietro Mosca[1], Chiara Groppo[2], and Franco Rolfo[1,2]**

[1]CNR – Istituto di Geoscienze e Georisorse, Unità di Torino, Via Valperga Caluso 35, I-10125, Torino, Italy

[2]Dipartimento di Scienze della Terra,

Università di Torino, Via Valperga Caluso 35, I-10125, Torino, Italy

*(*Email:p.mosca@csg.to.cnr.it)*

ABSTRACT

Structural-petrographic studies based on geological mapping were performed at the western flank of the Kangchenjunga massif, where the Lesser Himalayan Sequence (LHS) is exposed as a regional antiform (the Taplejung Window) beneath the Greater Himalayan Sequence (GHS), the latter being divided in the lower Inverted Metamorphic Sequence (IMS) and the upper Higher Himalayan Crystallines (HHC).

The juxtaposition of the high-grade mid-crustal HHC over the low- to medium-grade LHS is structurally recorded by the Main Central Thrust Zone (MCTZ), roughly equivalent to the IMS and typically showing a persistent top-to-the-south sense of regional thrusting. The boundaries of the MCTZ are not identifiable by single thrusts or by lithological contacts, but they are envisaged as zones of high strain localization. The lower boundary of the MCTZ is marked by phyllonites and mylonitic schists in the uppermost portions of the LHS near to the contact with the strongly mylonitic augen gneisses of the IMS. The upper boundary of the MCTZ is roughly located at the base of the Grt-Kfs-Ky-Sil anatectic gneiss (Barun-type) in the lower portion of the HHC, characterized by ductile shearing and boudinage. The thickness of the MCTZ ranges from 6-7 km in the north-western sector to 3-4 km in the south-eastern sector of the studied area. The overprinting of late foldings, mainly N to NE – S to SW and WNW-ESE striking, is likely responsible for the regional doming geometry of the investigated area.

Southward thrusting and dome formation could have been also favoured by the activity of high-angle, NE-SW striking brittle to brittle-ductile shear zones, such as the one observed in the Yampudin area.

Keywords: Structural acchitecture, tectono-metamorphic evolution, Kangchenjunga trasnsect, Himalaya

Received: 5 January 2011 **revision accepted:** 11 April 2011

INTRODUCTION

The Himalayan orogen developed after the India-Eurasia continental collision since 55 Ma (Garzanti et al. 1987; Rowley 1996). Traditionally, four E-W trending fault-bounded lithotectonic domains are distinguished (Fig. 1): from south to north and from lower to upper structural levels these are the Sub-Himalaya (or Siwalik Molasse Sequence), the Lesser Himalayan Sequence (LHS), the Greater Himalayan Sequence (GHS) and the Tibetan Sedimentary Series (TSS) (Gansser 1964; Le Fort 1975; Upreti 1999; Goscombe et al. 2006; Searle et al. 2008).

The Lesser Himalayan Sequence is bounded by the Main Boundary Thrust (MBT; Gansser 1964, 1981) at its bottom to the south and by the Main Central Thrust (MCT; Searle et al. 2008 for a review) at its top to the north (Fig. 1). The LHS consists mainly of low- to medium-grade metasediments (metapelitic schists and quarzites) associated with granitic orthogneiss (for a detailed review, see for instance Goscombe et al. 2006, McQuarrie et al. 2008 and Khon et al. 2010 and references therein).

The Greater Himalayan Sequence is bounded to the south by the MCT (as originally defined by Gansser 1964) and to the north by the South Tibetan Detachment System (STDS; Carosi et al. 1998, Kellet et al. 2010). From lower to upper structural levels, the GHS consists of: (i) medium- to high grade metasediments and granitic orthogneisses defining an Inverted Metamorphic Sequence (IMS), its metamorphic grade increasing structurally upward from the staurolite zone to the sillimanite zone and, locally, to anatexis (Goscombe et al. 2006; Groppo et al. 2009, 2010). This IMS roughly coincides with the Main Central Thrust Zone as defined by Goscombe et al. (2006). According to some authors the IMS is bounded at its top by a structural discontinuity (MCT of Bordet 1961; High Himal Thrust – HHT - of Goscombe et al. 2006, see Fig. 1 and the following discussion); (ii) high-grade gneiss, often anatectic, hosting networks and lens-shaped bodies of two-micas and tourmaline-bearing leucogranites, which can be as thick as 1-2 km at Mts. Makalu and Baruntse (Visonà and Lombardo 2002). These high-grade gneisses are known as Higher Himalayan Crystallines (HHC) (Fig. 1) and are characterized by a progressive decrease in peak-pressure

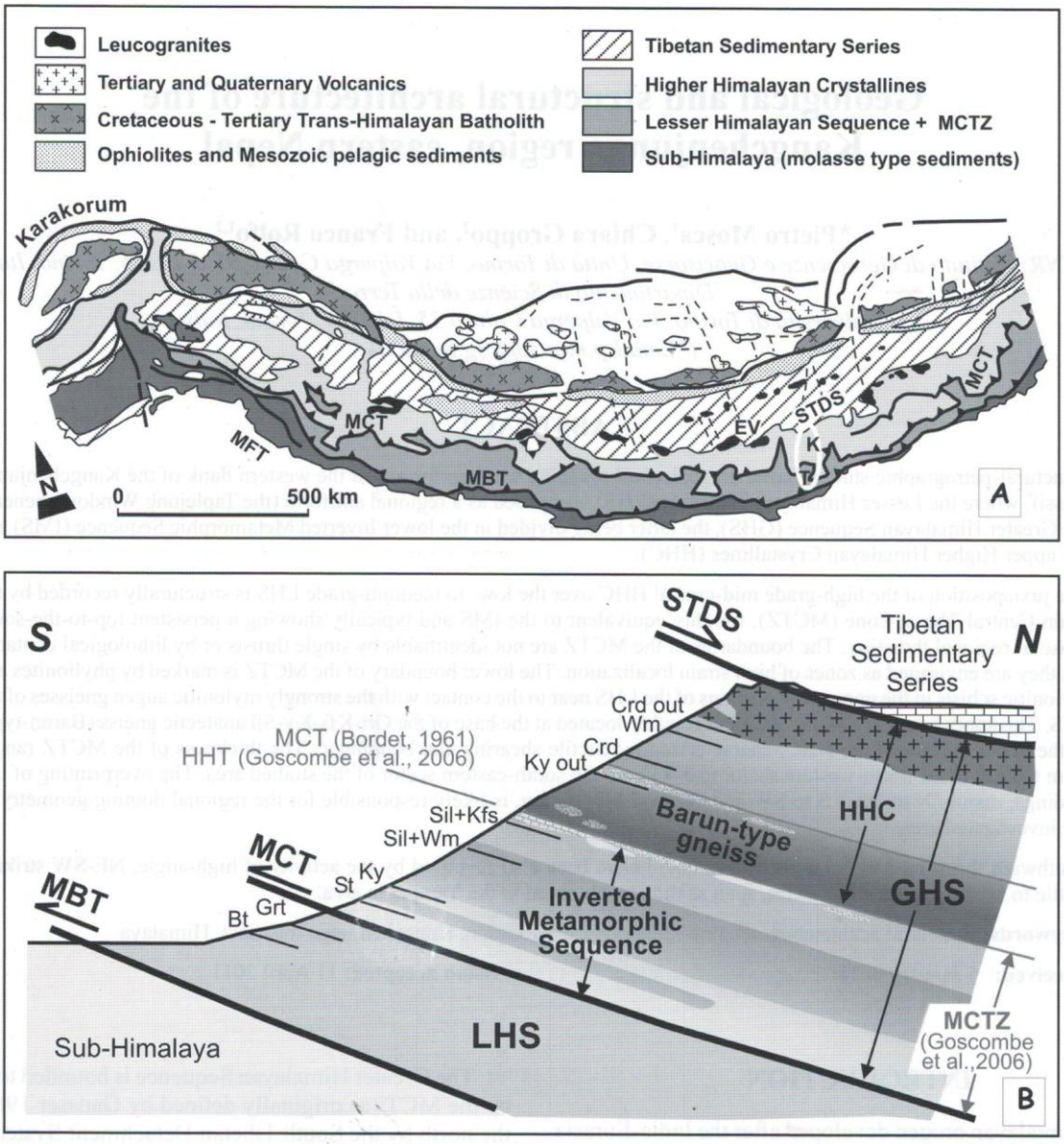

Fig. 1: (A) Simplified tectonic sketch map of the Himalaya, showing the main lithotectonic division and trace of the regional structures. The investigated area is outlined by the white ellipse. (B) Schematic cross-section across the eastern Himalaya (modified from Goscombe et al. 2006 and Searle et al. 2008). EV, Everest; HHT, High Himal Thrust; K, Kangchenjunga; LHS, Lesser Himalayan Sequence; MBT, Main Boundary Thrust; MCT, Main Central Thrust; MCTZ, Main Central Thrust Zone; MFT, Main Frontal Thrust; STDS, South Tibetan Detachment System; T, Taplejung. Mineral abbreviations for isograds are after Whitney and Evans (2010).

structurally upward (Pognante and Benna 1993; Lombardo et al. 1993; Davidson et al. 1997; Hodges 2000; Groppo et al. submitted).

The Tibetan Sedimentary Series overlie the HHC along the STDS and consist of Upper Precambrian to Eocene sediments originally deposited on the Indian continental margin (Gaetani and Garzanti 1991).

One of the most intriguing and long-time discussed geologic features of the Himalaya is the localization and interpretation of the tectonic juxtaposition of the GHS over the LHS, namely the IMS (or MCTZ of Goscombe et al. 2006). A number of studies (Searle et al. 2008 for a review) documented that shearing related to the GHS thrusting is not concentrated along a single surface and is characterized by a top-to-south sense of movement. However, an univocal interpretation of the MCTZ is still lacking.

Based on new structural and petrographic observations, the aim of this paper is to describe the geological architecture and the relationship between the LHS and GHS exposed

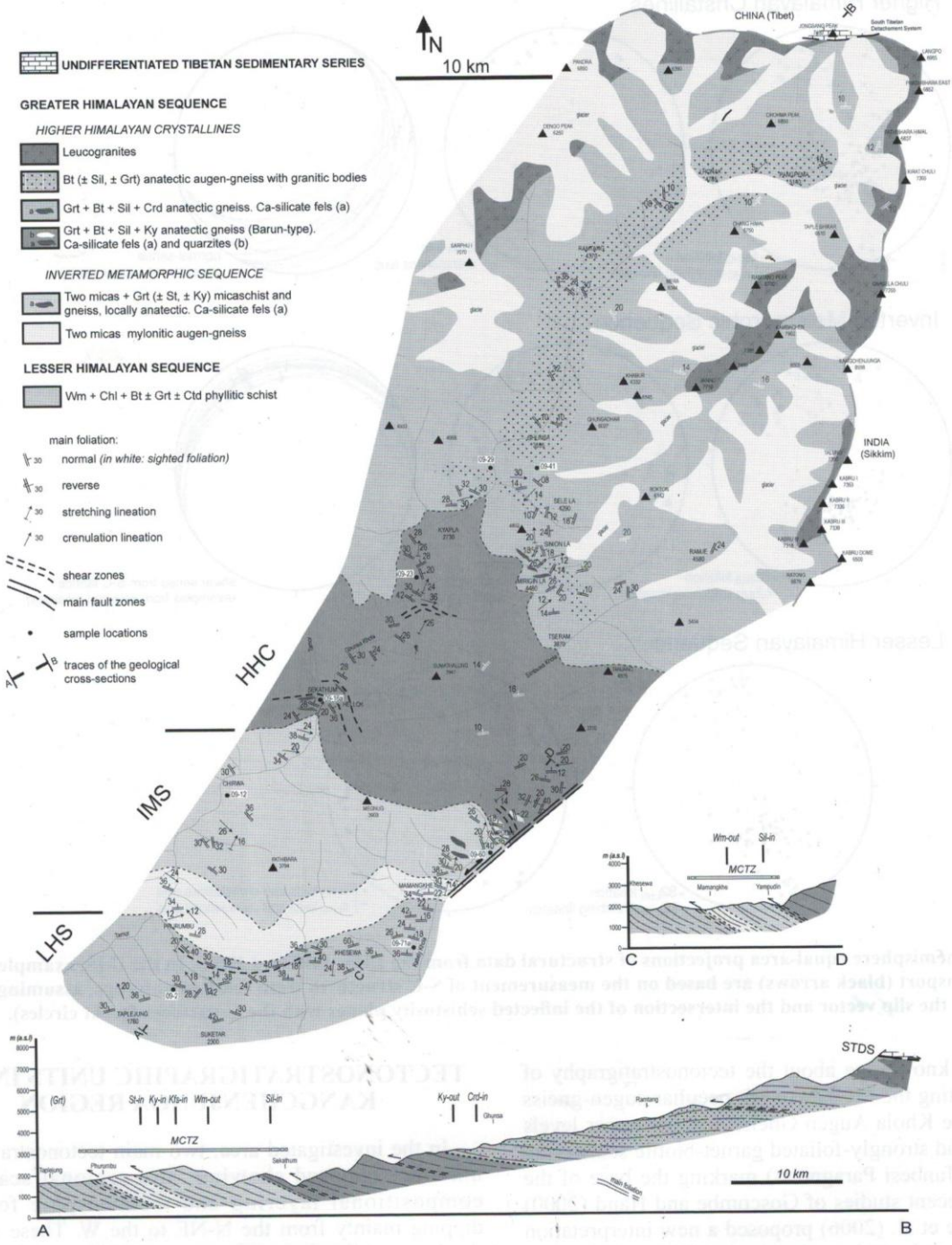

Fig. 2: Geological map and cross-sections of the western Kangchenjunga region in eastern Nepal based on the present study. Data for the northernmost sector along the Nepal-China border are from Goscombe et al. (2006).

in the Himalayan thrust belt of far-eastern Nepal, at the western flank of the Kangchenjunga massif, the easternmost Himalayan eight-thousander. Geological mapping, structural and petrographic data are reported (Fig. 2) and described along the Tamor-Ghunsa Khola and Simbuwa-Kabeli Khola, following two cross-sections in the northern and north-eastern flanks of the Taplejung tectonic Window (Tamor Khola window: Schelling and Arita 1991), where the LHS is exposed as a regional antiformal structure beneath the IMS and the HHC.

The main geologic framework of the investigated area can be envisaged in the map proposed by Shresta et al. (1984). Schelling and Arita (1991) and Schelling (1992) significantly

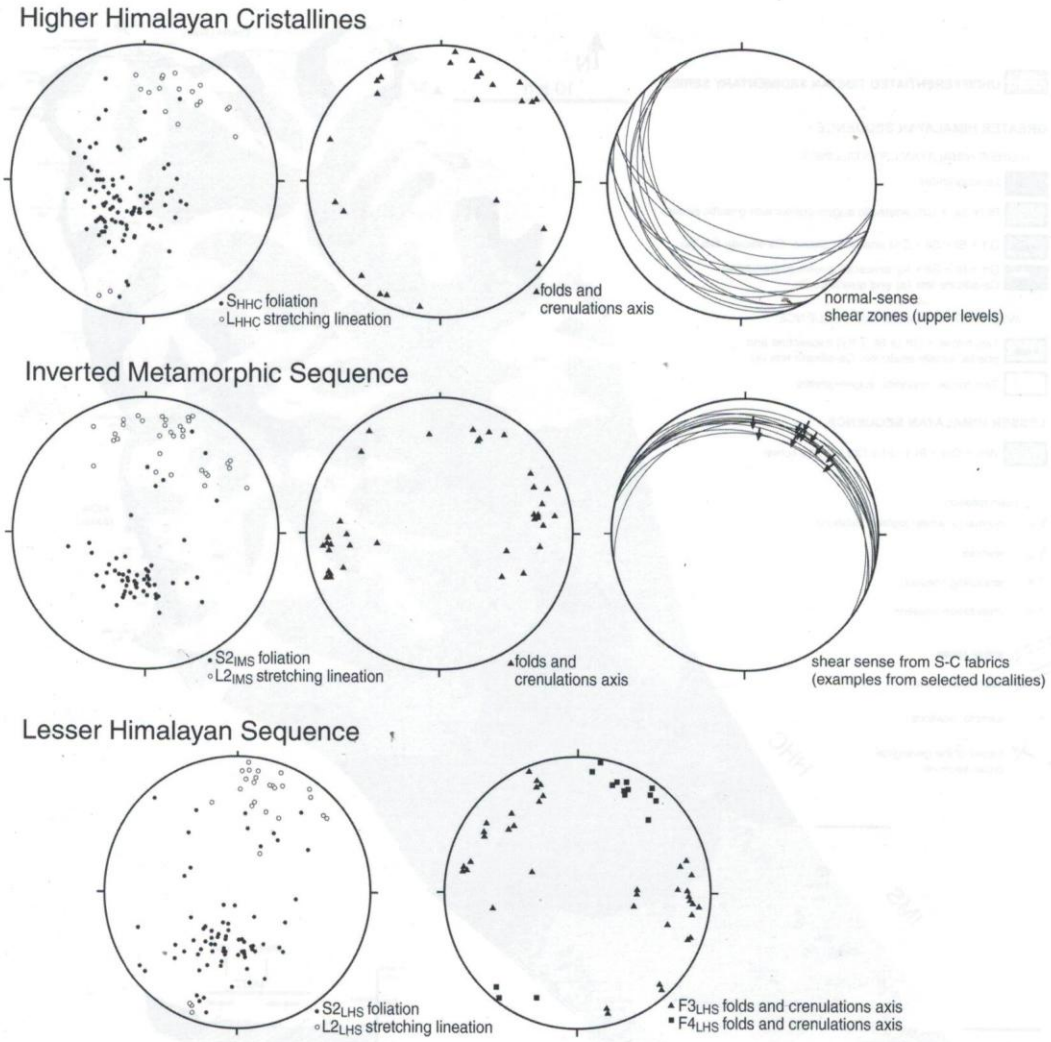

Fig. 3: Lower hemisphere equal-area projections of structural data from the LHS, IMS and HHC. In the IMS, examples of sense of tectonic transport (black arrows) are based on the measurement of S-C structures from selected outcrops, assuming an angle of 90° between the slip vector and the intersection of the inflected schistosity planes with the C-surfaces (great circles).

improved the knowledge about the tectonostratigraphy of this area, locating the MCT between peculiar augen-gneiss – i.e. the Sisne Khola Augen Gneiss – at the upper levels of the LHS, and strongly-foliated garnet-biotite schists and gneisses (the Junbesi Paragneiss) marking the base of the HHC. More recent studies of Goscombe and Hand (2000) and Goscombe et al. (2006) proposed a new interpretation of the local tectonic setting, placing the MCT at the base of the Sisne Khola Augen Gneiss. These authors emphasized that the orogen architecture in eastern Nepal was mainly controlled by the HHT, a regional shear zone within the GHS. The HHT separates a lower-plate, characterized by a penetrative transposed planar schistosity, from an upper-plate, showing more complex internal structural geometries and different migmatite generations. A recent petrologic study in eastern Nepal by Imayama et al. (2010) discusses a metamorphic P-T profile across the western portion of the area described in this paper.

TECTONOSTRATIGRAPHIC UNITS IN THE KANGCHENJUNGA REGION

In the investigated area, two main tectonostratigraphic units are exposed showing, at a regional scale, both compositional layering and metamorphic foliations dipping mainly from the N-NE to the W. These units are the Lesser Himalayan Sequence (LHS) and the Greater Himalayan Sequence (GHS) (Fig. 2), the latter being further subdivided into the lower Inverted Metamorphic Sequence (IMS) and in the upper Higher Himalayan Crystallines (HHC). Lithological and structural features (Fig. 3) of each tectonostratigraphic unit are in the following reported from south to north, i.e. from the lower to the upper structural levels. Subscript acronyms LHS, IMS and HHC refer respectively to the geological features identified in the Lesser Himalayan Sequence, Inverted Metamorphic Sequence and Higher Himalayan Crystallines. Mineral abbreviations are after Whitney and Evans (2010).

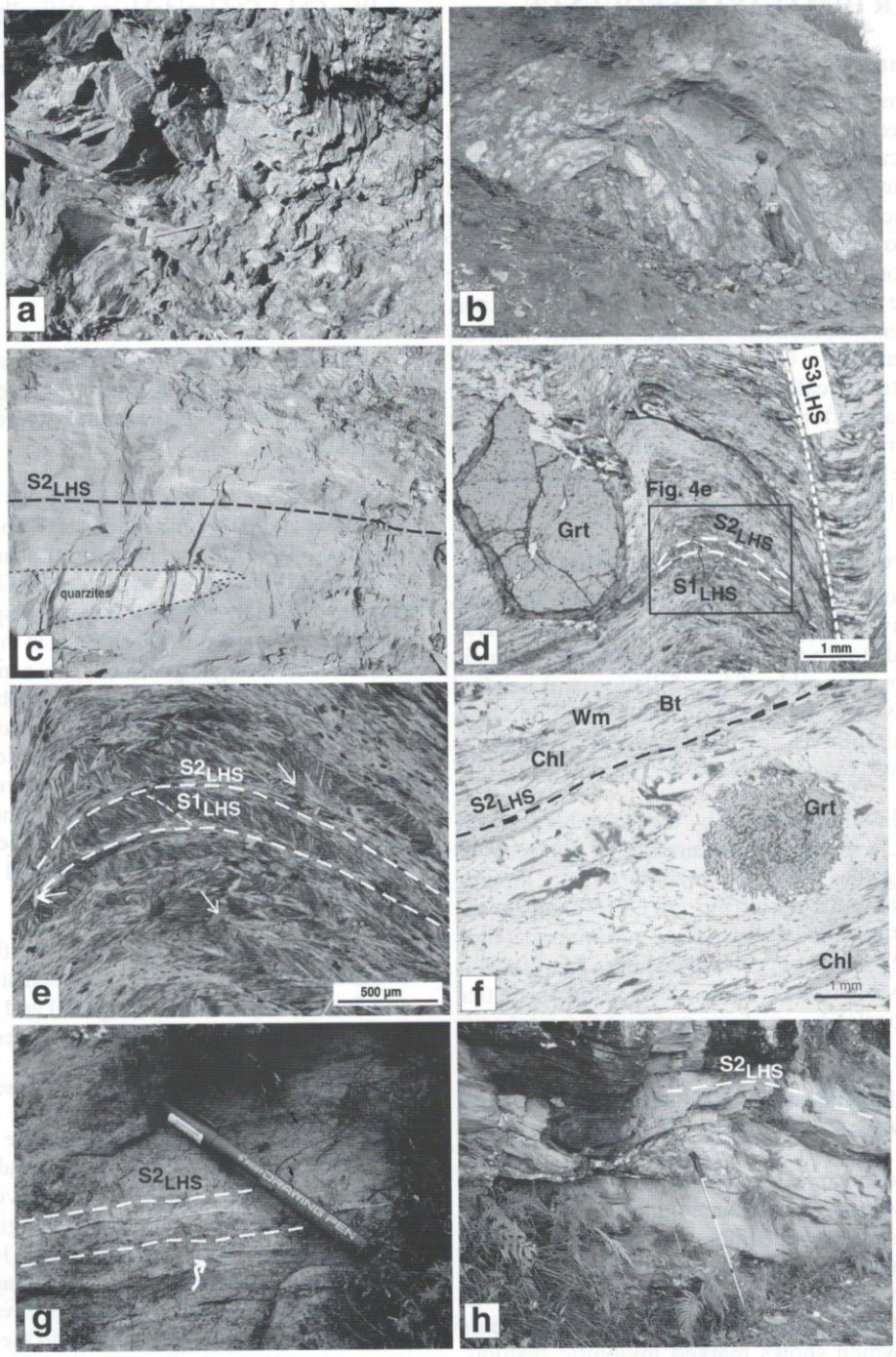

Fig. 4: Meso- and micro-structural features of Lesser Himalayan Sequence lithologies. (a) Pale-green fine-grained slates, representing the most common lithology of the LHS. (b) Chlorite-sericite schists intercalated in the more abundant quartz-sericite schists and affected by later folding with sub-vertical axial plane. (c) Cm-scale intercalations of Grt-Amp quartzite within LHS slates. (d) Photomicrograph showing the main $S2_{LHS}$ foliation in a quartz-sericite schist (sample 09-2; Plane Polarized Light, PPL). $S2_{LHS}$, defined by Wm + Chl + minor Bt, is deformed by a $F3_{LHS}$ phase responsible for the development of asymmetric crenulation. The axial planar foliation of these $F3_{LHS}$ folds ($S3_{LHS}$) consists of Wm + Bt. (e) Detail of (d) showing the main foliation $S2_{LHS}$ transposing an older $S1_{LHS}$ foliation defined by Wm + Chl. Late Wm and Bt flakes statically overgrowing the $S2_{LHS}$ are also locally evident (white arrows) (PPL). (f) Photomicrograph showing pre- $S2_{LHS}$ garnet porphyroblast in a garnet-bearing schist (sample 09-71a; PPL), with a rotated internal schistosity defined by quartz. The main foliation ($S2_{LHS}$) is defined by Wm + Bt. Large chlorite flakes are statically overgrown on the $S2_{LHS}$ (PPL). (g) Example of cm-scale intrafolial fold (white arrow) between $S2_{LHS}$ surfaces. (h) Internal south-directed thrusting in the LHS.

LESSER HIMALAYAN SEQUENCE

Lithological features

The LHS consists of a monotonous series of grey to pale-green fine-grained quartz-sericite schists, slates and phyllites (Fig. 4a), intercalated with metric-scale levels of either massive quartzites (± Grt ± Ctd) or chlorite-sericite schists (Fig. 4b). Cm-scale intercalations of Grt-Amp quartzites (Fig. 4c) are also observed in the upper structural levels of the LHS. At the outcrop scale, quartzites are generally better exposed than the fine-grained sericite-schists and phyllites, but they are often monotonous and lack of index minerals (except for the rare Grt + Ctd). On the contrary, schists and phyllites are petrologically more informative: millimetric garnet crystals are often evident on the hand sample as well as coarse-grained biotite flakes overgrowing the main foliation (Fig. 4e). Graphite-rich schists occur locally in the lower structural levels.

Meso- and micro- structures and deformation records

Both at the outcrop and thin-section scales, the LHS schists are intensively folded and crenulated. The main planar fabric corresponds to a pervasive $S2_{LHS}$ foliation. This main foliation transposes an older $S1_{LHS}$ foliation and original compositional layering. $S1_{LHS}$ foliation is defined by Qtz + Wm ± Chl in microlithons, and by inclusion trails of Qtz in Grt porphyroblasts (Figs. 4d, 4e and 4f).

The $S2_{LHS}$ foliation is defined by the assemblage Qtz + Wm ± Chl ± Bt, with the rare occurrence of syn-tectonic snowball Grt (Fig. 4f). The $S2_{LHS}$ foliation, usually dipping at a regional scale to the north (Fig. 3), corresponds to the axial planar foliation of locally preserved asymmetrical tight south-verging $F2_{LHS}$ folds; occurrence of intrafolial folds is due to the progressive intensive shearing (Fig. 4g), such that the older lithological/ $S1_{LHS}$ surfaces merge in the composite $S2_{LHS}$ surface.

A $L2_{LHS}$ stretching lineation is defined by aligned Wm, Bt and Qtz, and is always almost parallel to the $S2_{LHS}$ dip (Fig. 3).

The uppermost structural levels of the LHS (approximately 500-800 m below the mylonitic augen-gneisses of the IMS) consist of a peculiarly strained domain exhibiting a strong increase in deformation degree. There, all lithologies show usually a phyllonitic-mylonitic aspects and low-angle ductile-brittle to brittle shear zones locally occur parallel to the main $S2_{LHS}$ foliation, which shows marked mylonitic features. S-C fabrics and thrusting with top-to-south movements are evident at the outcrop scale (Fig. 4h).

The $S2_{LHS}$ is deformed by at least two major phases ($F3_{LHS}$ and $F4_{LHS}$) of later folding (Fig. 3). Asymmetric $F3_{LHS}$ folds and crenulations have sub-horizontal hinges trending from W-E to NW-SE, roughly orthogonal to the $L2_{LHS}$, and show south-vergence. The axial planar foliation of these folds ($S3_{LHS}$) is only locally well developed (Fig. 4d) and mainly consists of Wm ± Bt. In most of the lithologies, however, Wm + Bt ± Chl ± Ctd lepidoblasts statically overgrow the $S2_{LHS}$ (Fig. 4e), without a well developed $S3_{LHS}$. Open to chevron $F4_{LHS}$ folds and crenulations are characterized by N-S to NNE-SSW trending hinges moderately plunging north and by sub-vertical axial planes.

GREATER HIMALAYAN SEQUENCE

Inverted Metamorphic Sequence

Lithological features

The IMS comprises rock-types characterized by a distinct inverted metamorphism, and is the strongly condensed and thinned equivalent of the MCTZ as defined by Goscombe et al. (2006).

At structurally lower levels of this sequence, two mica mylonitic augen-gneisses (Sisne Khola Augen Gneiss of Schelling 1992) are well exposed near the Phurumbu and Mamangke villages (along the Tamor-Ghunsa Khola and the Simbuwa-Kabely Khola transects, respectively), and their thickness range from 1500-2000 m in the west to <1500 m in the east. These augen gneisses show a mylonitic texture with large (often > 2-3 cm) K-feldspar porphyroclasts enveloped by the main mylonitic foliation defined by Wm + Bt (Figs. 5a and 5b). Intercalations of meter-scale chloritic schists are observed as well as small mafic enclaves elongated parallel to the main foliation. According to their petrography and structural position, these augen-gneisses may be correlated to the Ulleri Gneisses of central Nepal (e.g. Le Fort, 1975; Arita, 1983).

Moving upwards, a few kilometer-thick unit consists of two micas + Grt (± St ± Ky ± Kfs) schist and gneiss (Figs. 5c and 5e), locally anatectic (Fig. 5d) and hosting metre-thick bodies of calc-silicate fels and quarzites.

Meso- and micro-structures and deformation records

The prominent planar fabric of the IMS is a mylonitic $S2_{IMS}$ foliation (Figs. 5a, 5c, 5f, 5g and 5h) resulting from high strain, which led to an intensive transposition and parallelization of the original lithological layering and of an older metamorphic foliation ($S1_{IMS}$) (Fig. 5f). Relicts of $S1_{IMS}$ are also preserved as inclusions trails of Qtz + Rt in Grt porphyroclasts, which are generally enveloped by the $S2_{IMS}$. $S2_{IMS}$ foliation, dipping uniformly to the north, is defined by Wm + Bt ± Ky ± St (Fig. 5e) and, at the outcrop scale, it corresponds to the axial plane foliation of $F2_{IMS}$ isoclinal to tight folds with south-vergence. Intrafolial folds are also often identifiable. A pervasive mineral and elongation lineation (Fig. 3) is defined by the preferred alignment of minerals or mineral aggregates (Bt, Wm, St and Ky) in the schists and by stretched K-feldspar porphyroclasts in the augen-gneisses. The orientation of the stretching lineation is always parallel or slightly oblique to the dip-direction of the $S2_{IMS}$ foliation.

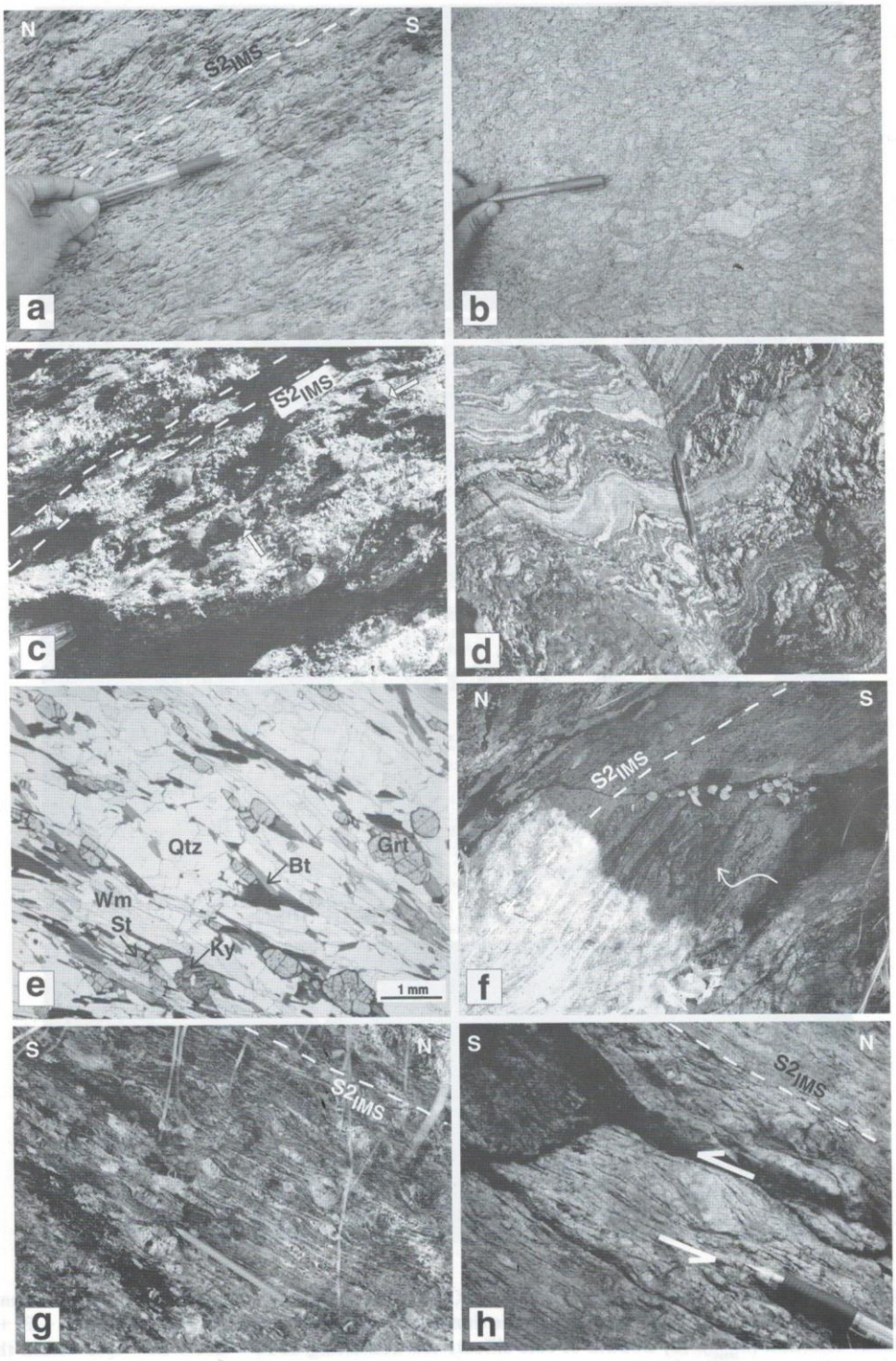

Fig. 5: Meso- and micro-structural features of Inverted Metamorphic Sequence lithologies. (a) Typical aspect of the two micas mylonitic augen gneiss: the large K-feldspar porphyroclasts are enveloped by the main foliation ($S2_{IMS}$) defined by Wm + Bt. (b) Less deformed portion of the two micas augen-gneiss, characterized by a less pervasive $S2_{IMS}$ foliation. (c) Detail of a two micas Grt-, St-, Ky-bearing schist. Note the garnet (white arrows) enveloped by the main foliation $S2_{IMS}$, defined by Wm + Bt. (d) Two micas Grt-bearing anatectic gneiss, consisting of quartzo-feldspathic domains alternating with mica-rich darker layers. (e) Photomicrograph showing two micas Grt-, St-, Ky-bearing schist (sample 09-12; PPL). The main foliation $S2_{IMS}$ is defined by Wm + Bt. (f) Transposition of lithological boundaries (white arrow) by $S2_{IMS}$ mylonitic foliation. (g) Strongly foliated augen gneiss with top-to-the-south sense of shear. (h) Examples of a cm-scale K-feldspar porphyiroclast marking top-to-the-south sense of shear.

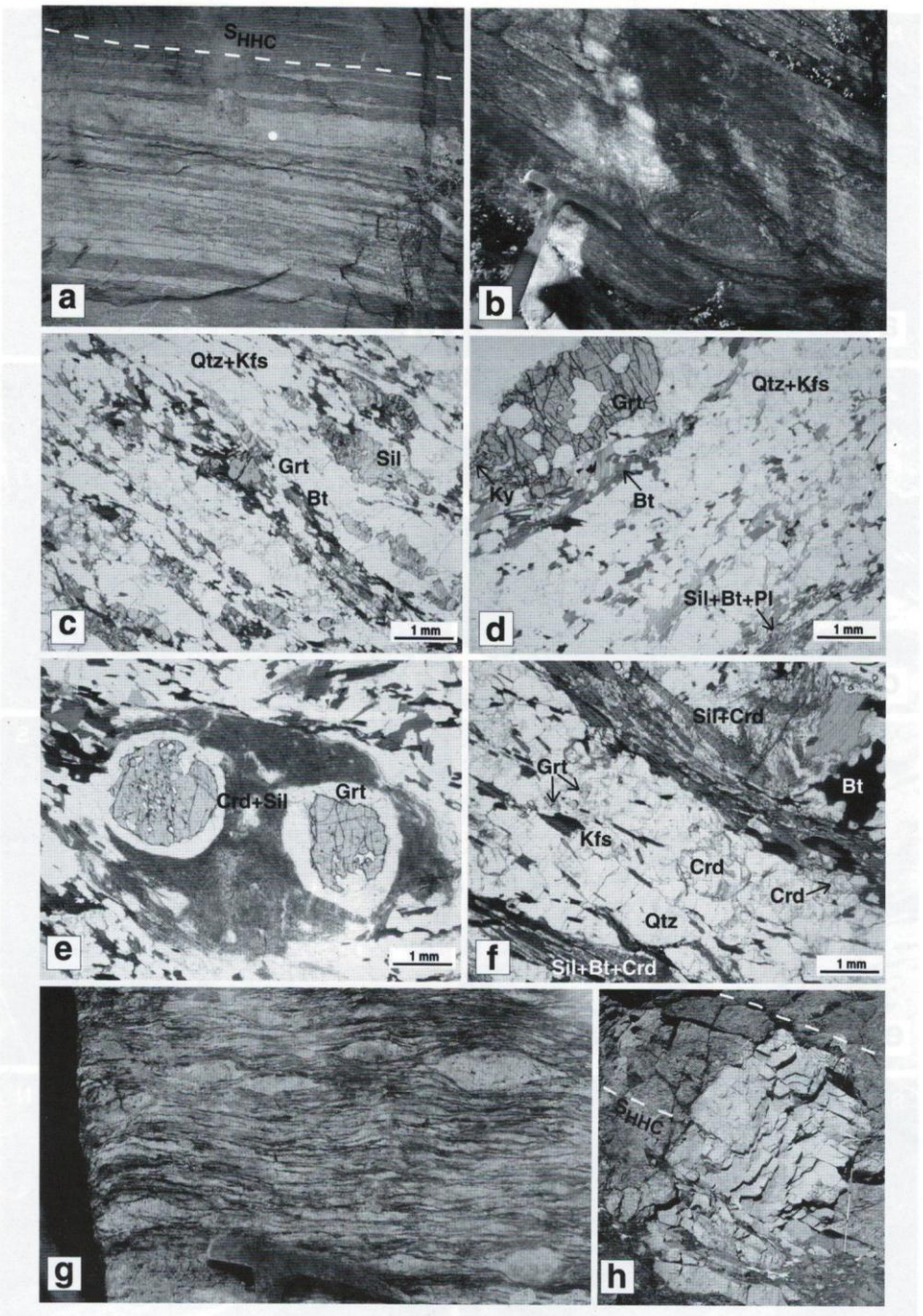

Fig. 6: Meso- and micro-structural features of Higher Himalayan Crystallines lithologies. (a) Grt + Kfs + Ky + Sil anatectic paragneiss ("Barun type") consisting of quartzo-feldspathic leucocratic domains alternating with millimetric dark Bt + Pl + Sil ± Grt layers which define a planar foliation (S_{HHC}). (b) Boudin of calc-silicate fels consisting of Pl + Grt + Di + Qtz within the "Barun type" anatectic paragneiss and enveloped by the main S_{HHC} foliation. (c, d) Photomicrographs showing representative microstructures of the Grt + Kfs + Ky + Sil anatectic paragneiss (c: sample 09-23; d: sample 09-16a; PPL). The leucocratic domains mainly consist of Qtz and Kfs, whereas the darker layers are defined by Bt + Sil + Pl. The Grt porphyroblast in (d) includes relict Ky and large polymineralic inclusions of Qtz + Pl. (e, f) Photomicrographs showing representative microstructures of the Crd-bearing anatectic paragneiss occurring at the upper structural levels of HHC (e: sample 09-41; f: sample 09-29; PPL). Crd + Sil + Bt dark layers define the main foliation S_{HHC} and are alternated with quartzo-feldspathic leucocratic domains (f). Note the Crd + Sil corona replacing garnet porphyroblasts in (e). (g) Sil-bearing anatectic orthogneiss associated to the Crd-bearing paragneiss and characterized by a mylonitic fabric, with Kfs porphyroclasts highly stretched and rotated along the S_{HHC} foliation. (h) Tourmaline-bearing granitic dyke crosscutting the mylonitic S_{HHC} foliation in the Sil-bearing anatectic orthogneiss.

Mylonitic augen-gneisses occur in the lowermost structural levels of the IMS, along the contact with the schists and phyllites of the LHS (Fig. 5a). Due to the intensive shear which led to the development of the pervasive $S2_{IMS}$ composite foliation, less deformed or undeformed granitic portions can be only locally observed (Figs. 5a and 5b). At the outcrop scale, abundant K-feldspars with s-type geometries (Figs. 5a and 5h) and S-C fabrics are observed, with development of cm- to m-scale shear zones almost parallel to the main $S2_{IMS}$ foliation. Geometries of kinematic indicators uniformly define a top-to-south sense of shear.

$S2_{IMS}$ foliation is mainly deformed by SSE-verging folds and crenulation, and by folds plunging gently north and with sub-vertical axial plane (Fig. 3).

HIGHER HIMALAYAN CRYSTALLINES

Lithological features

The HHC are exposed over more than 20 km of relative thickness up to STDS at the Tibetan border. The lower structural levels of the HHC consist of Grt + Kfs + Ky + Sil anatectic paragneiss (Fig. 6a) with intercalations and boudins of quarzite, impure marble and calc-silicate rock with an assemblage of Di + Pl + Qtz ± Grt ± Amp (Fig. 6b). These peculiar gneisses are reported in the literature as Rolwaling-Khumbu- Kangchenjunga Paragneiss (Schelling 1992) and Jannu-Kangchenjunga Gneiss (Goscombe et al. 2006), and are considered to be the lateral equivalents of the Barun gneiss occurring in the Everest-Makalu region (Lombardo et al. 1993; Groppo et al. 2012). At the outcrop scale, this lithology typically consists of millimetric to centimetric leucocratic domains rich in quartz and feldspar alternating with millimetric dark Bt + Pl + Sil layers which generally define a more or less continuous planar foliation (Fig. 6a). Garnet is always present and occurs as mm- to cm-scale porphyroblasts generally enveloped by the Bt + Pl + Sil foliation, or within the leucocratic domains (Figs. 6c and 6d). Kyanite occurs as a relict phase generally corroded by Pl ± Bt or included in the Grt (Fig. 6d).

The upper structural levels of the HHC consist of Grt + Bt + Sil + Crd anatectic paragneisses, which differ from the lower "Barun-type" gneiss for the lack of kyanite and the abundant occurrence of cordierite (Figs. 6e and 6f). These Crd-bearing paragneisses are associated to large bodies of sillimanite-bearing anatectic orthogneisses (Fig. 6g) and frequent tourmaline- and/or andalusite-bearing leucogranites. Above the 3500 m towards the Tibetan border, meter- to decameter-scale leucogranitic dykes and sills are observed (Fig. 6h). The leucogranitic bodies significantly increase in volume towards higher structural levels (Fig. 7a).

Meso- and micro-structures and deformation records

The prominent planar fabric in the HHC is represented by a penetrative S_{HHC} foliation parallel to the compositional layering (Fig. 6a and 7c). At a regional scale, S_{HHC} dips at moderate angle towards the north and the east (Fig. 3). The S_{HHC} foliation contains a stretching mineral lineation (L_{HHC}) defined by aligned Sil, Qtz and Bt and plunging almost parallel to the S_{HHC} dip (Fig. 3). Locally, the S_{HHC} is crosscut by granites and pegmatitic dykes (Fig. 6h).

The structurally lower levels of the HHC show evidence of pervasive ductile shearing associated to the development of the S_{HHC}: in particular, S-C fabrics and s-type Kfs porphyroclasts define a top-to-south sense of shear. In addition, the development of the pervasive shearing is accompanied by intensive boudinage of calc-silicate fels and marbles. At the lowermost structural levels of the HHC, immediately above the IMS, the Grt + Kfs + Ky + Sil anatectic paragneiss locally shows meter- to decameter-scale shear zones discordant with the S_{HHC} foliation (Fig. 7c). These shear zones are characterized by a significant grain reduction and a penetrative low-grade metamorphic foliation.

In the structurally upper levels of the HHC, the Sil-bearing anatectic orthogneisses are often characterized by mylonitic fabric (Fig. 6g). Kfs porphyroclasts are highly stretched and rotated along the S_{HHC} foliation, defining a marked L_{HHC}. S-C fabrics are variably recognizable in centimetre- to decimeter-scale discrete shear zones, gently dipping to the north and showing top-to-south tectonic transport.

Locally at the upper structural levels of the HHC, the main S_{HHC} foliation is cross-cut at high angle by cm -scale S to SW-dipping normal-sense shear zones (Fig. 7b).

The S_{HHC} foliation is deformed by several mesoscopic folds (Fig. 3). Most of them comprise asymmetric tight to isoclinal folds, with fold axes plunging gently to the NE and SW, and axial planes being sub-horizontal or dipping toward the NW (Fig. 7d). Peculiar SSE-verging folds with moderately SSE-dipping axial planes (Fig. 7e) occur in the Yampudin-Mirgin La area; their development could be associated with a shear zone running along the Kabeli Khola in the Yampudin area (see the following discussion).

BRITTLE STRUCTURES

Throughout the mapped area, all metamorphic foliations are intersected by late brittle faults and abundant joints. Field data point the persistence of a NE-SW fault system at a regional scale. In particular, a number of m- to dam-scale fault zones are observed in the middle–upper structural levels of the HHC. These are identified by high angle, closely spaced surfaces, variably dipping to the south-eastern or north-western sectors, and often characterized by normal displacements. The most important NE-SW trending fault

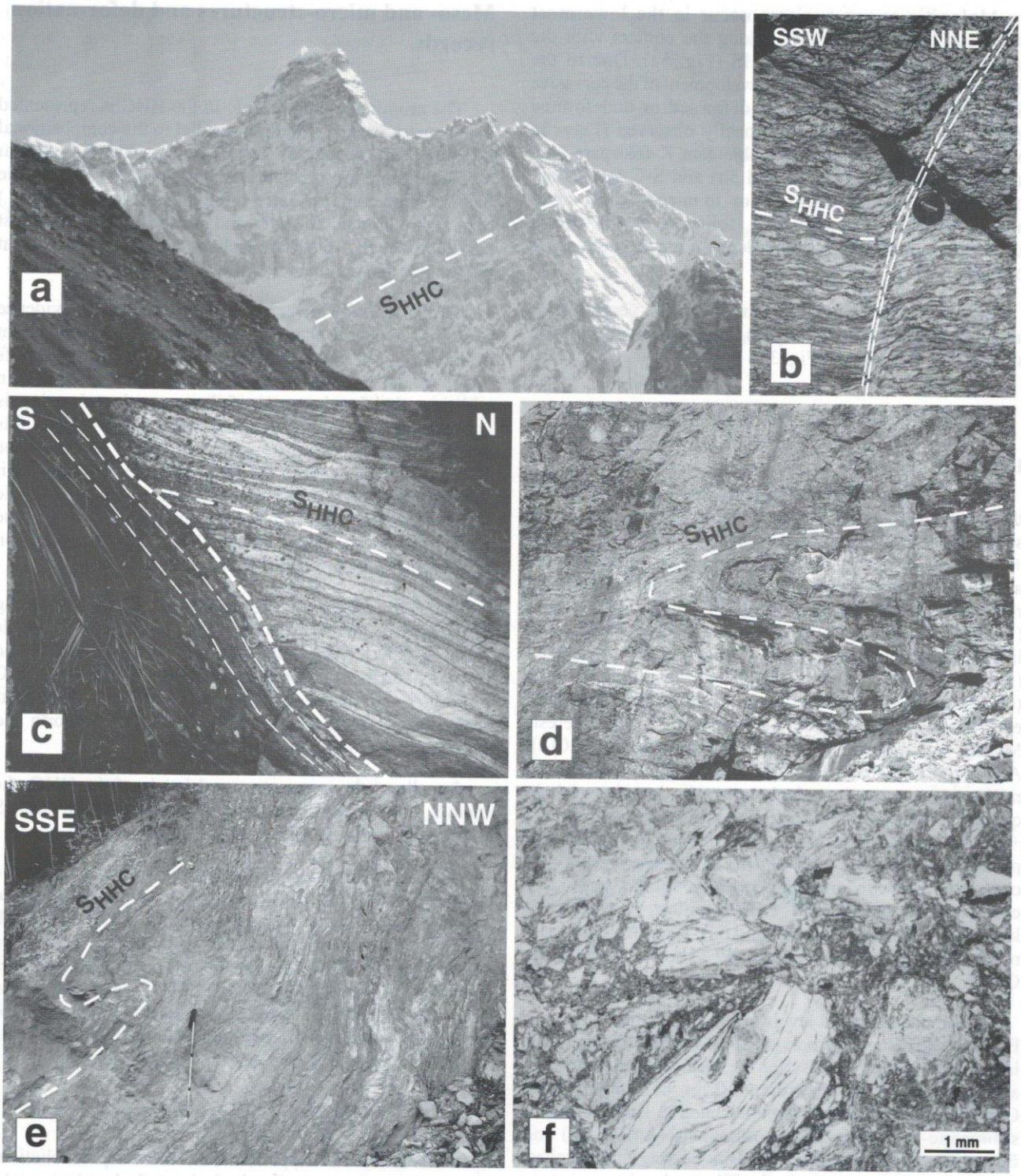

Fig. 7: (a) West face of Mt. Jannu (7710 m) showing the significant increase of leucogranites in the higher structural levels of the HHC. (b) Cm-scale extensional shear zones in the Sil-bearing orthogneiss from the upper structural level of the HHC. (c) Shear zone cutting the S_{HHC} foliation in the "Barun-type" paragneiss from the lower structural levels of the HHC. (d) Example of late folds with low-angle north-dipping axial plane in the HHC gneiss exposed in the Mirgin La area. (e) SSE-verging folds affecting Bt + Sil gneiss in the Yampudin area. (f) Photomicrograph showing microstructures of cataclasites derived from quartzites within the brittle shear zone in the Yampudin area (sample 09-60; PPL).

zone is recognized in the Yampudin area along the Kabely Khola, at the south eastern side of the mapped area. It is identified by a network of brittle discontinuities, often having strike-slip indicators, and it is marked by the occurrence of abundant cataclasites derived from gneiss and quartzites (Fig. 7f).

DISCUSSIONS AND CONCLUSIONS

The structural architecture of the Himalayas in the studied area is dominated by north-dipping composite foliations and tectonic contacts, parallel to the lithological contacts or compositional banding. This apparently simple configuration is the result of a high-strain and protracted deformational history, recorded in all the mapped tectonostratigraphic units by the widespread transposition of older schistosities and lithological boundaries, by the development of ductile to brittle-ductile shear zones and by the complex overprinting by late folding and crenulations.

The tectonic juxtaposition of the high-grade mid-crustal HHC over the low- to medium-grade metasedimentary LHS is structurally recorded by the MCTZ (sensu Goscombe et al. 2006), here corresponding to a ductile to ductile-brittle shear zone roughly centred on the IMS. In the studied area, the boundaries of the MCTZ are not simply identified by a single thrust or a set of adjacent, minor thrusts, or by lithological contacts, but they are envisaged as zones of high strain localization (i.e. marking an increase in the intensity of the deformation). The lower boundary of the MCTZ can be located in the phyllonites and mylonitic schists of the uppermost portions of the LHS near to the contact with the foliated augen-gneisses, which are in turn characterized by a widespread stretching of K-feldspar porphyroclasts. The upper boundary of the MCTZ can be roughly located at the base of the "Barun-type" gneiss (i.e. the lower portion of the HHC), characterized by evidence of pervasive ductile shearing (meso-scale shear zones with top-to-south sense of movements and isoclinal folding) and boudinage. Moving structurally upwards, through the middle-upper portions of the HHC, ductile high-strain is often concentrated along discrete, top-to-south meter to decametre-scale shear zones. On the basis of this observation, the thickness of the MCTZ ranges from 6-7 km in the north-western portion to 3-4 km in the south-eastern portion of the studied area.

In the MCTZ, shear zones are quite common from microscopic- to mesoscopic scale and their general aspect is controlled by several parameters, such as the difference and contrast in rheological properties between different lithologies, the presence of rigid objects (porphyroclasts) and the occurrence of pre-existing planar anisotropies. The abundant kinematic indicators mark uniform top-to-south sense of regional thrusting. This direction is also confirmed by pervasive stretching lineations defined by minerals or porphyroclasts alignments, parallel or slightly oblique to the dip-direction of the main mylonitic foliation.

The overprinting of late folding, axes of which striking mainly N to NE – S to SW and WNW-ESE, is likely responsible for the doming at a regional scale, thus leading to the exposure of the LHS below the IMS and the HHC in the Taplejung window.

During the tectonic evolution of the western Kangchenjunga region, an important role could have been played by the shear zone observed in the Yampudin area, interpreted as a brittle to brittle- ductile shear zone as suggested by the presence of brittle discontinuities and asymmetric folds. This structure, could have favoured lateral (probably dextral) movements during the regional southwards thrusting, acting similarly to a lateral ramp and causing a variation of the thickness of the MCTZ, and/or it was active during the stages of the regional dome formation.

As concerning the extensional movements locally observed at the upper portion of the HHC, they could be associated to the regional extension occurring along the STDS.

ACKNOWLEDGEMENTS

Fieldwork was carried out thanks to contributions from the CNR-IGG, UO Torino (P.M. and F.R.) and from PRIN Cofin 2006 and ex-60% founds (C.G. and F.R.). Attendance to the NGS Congress was financially supported by Ev-K2-CNR in collaboration with the Nepal Academy of Science and Technology as foreseen by the Memorandum of Understanding between Nepal and Italy, and thanks to contributions from the Italian National Research Council and the Italian Ministry of Foreign Affairs. Three anonymous reviewers are gratefully acknowledged for their constructive comments.

REFERENCES

Arita, K., 1983, Origin of the inverted metamorphism of the Lower Himalayas, Central Nepal. Tectonophysics, v. 93, pp. 43-60.

Bordet, P., 1961, *Recherches géologiques dans l'Himalaya du Népal, région du Makalu.* Editions du Centre National de la Recherche Scientifique, Paris, 275 p.

Carosi, R., Lombardo, B., Molli G., Musumeci, G., and Pertusati, P.C., 1998, The South Tibetan Detachment System in the Rongbuk valley, Everest region. Deformation features and geological implications. Jour. Asian Earth Sci., v. 16, pp. 299-311.

Davidson, C., Grujic, D. E., Hollister, L. S., and Schmid, S. M., 1997, Metamorphic reactions related to decompression and synkinematic intrusion of leucogranite, High Himalayan Crystallines, Bhutan. Jour. Metamorphic Geology, v. 15, pp. 593–612.

Gaetani, M. and Garzanti, E., 1991, Multiclycic history of the northern India continental margin (NW Himalaya). American Association Petroleum Geologists Bull. v. 75, pp. 1427-1446.

Gansser, A., 1964, *Geology of the Himalayas.* Wiley Interscience, New York, 289 p.

Gansser A., 1981, The geodynamic history of the Himalaya. American Geophysical Union, Washington, Geodynamics, Series 3, pp. 111-121.

Garzanti, E., Baud, A., and Mascle, G.., 1987, Sedimentary record of the northward flight of India and its collision with Eurasia (Ladakh Himalaya, India). Geodinamica Acta 1, pp. 297-312.

Goscombe, B. and Hand, M., 2000, Contrasting P-T paths in the Eastern Himalaya, Nepal: inverted isograds in a paired metamorphic mountain belt. Jour. Petrology, v. 41, pp. 1673–1719.

Goscombe, B., Gray, D., and Hand, M., 2006, Crustal architecture of the Himalayan metamorphic front in eastern Nepal. Gondwana Research, v. 10, pp. 232–255.

Groppo C., Rolfo F., and Indares A. Partial melting in the Higher Himalayan Crystallines of Eastern Nepal: the effect of decompression and implications for the "channel flow" model. *Submitted* to Jour. Petrology.

Groppo C., Rolfo F., and Indares A., 2012, Partial melting in the Higher Himalayan Crystallines of Eastern Nepal: the effect of decompression and implications for the "channel flow" model. Jour. Petrology, v. 53, pp. 1057-1088.

Hodges, K. V., 2000, Tectonics of the Himalaya and southern Tibet from two perspectives. Geol. Soc. America Bull., v. 112, pp. 324-350.

Imayama, T., Takeshita, T., and Arita, K., 2010, Metamorphic P–T profile and P–T path discontinuity across the far-eastern Nepal Himalaya: investigation of channel flow models. Jour. Metamorphic Geology, v. 28, pp. 527–549.

Kellett, D. A., Grujic, D., Warren, C., Cottle, J., Jamieson, R. and Tenzin, T., 2010,. Metamorphic history of a syn-convergent orogen-parallel detachment: The South Tibetan detachment system, eastern Himalaya. Journal of Metamorphic Geology 28, pp 785-808.Groppo, C., Rubatto, D., Rolfo, F., and Lombardo, B., 2010, Early Oligocene partial melting in the Main Central Thrust Zone (Arun Valley, eastern Nepal Himalaya). Lithos, v. 118, pp. 287–301.Kohn, M. J., Paul, S. K., and Corrie, S. L., 2010, The lower Lesser Himalayan sequence: A Paleoproterozoic arc on the northern margin of the Indian plate, 2010, GSA Bulletin, 122, 3/4, pp. 323–335, doi: 10.1130/B26587.1.

Le Fort, P., 1975, Himalaya: the collided range. Present knowledge of the continental arc. American Jour. Sci., v. 275A, pp. 1–44.

Lombardo, B., Pertusati, P., and Borghi, A., 1993, Geology and tectono-magmatic evolution of the eastern Himalaya along the Chomolungma-Makalu transect. In: Treloar, P.J. and Searle, M.P. (eds.) Himalayan Tectonics. Geol. Soc. London, Spec. Pub., v. 74, pp. 341–355.

McQuarrie, N., Robinson, D., Long, S., Tobgay, T., Grujic, D., Gehrels, G., and Ducea, M., 2008, Preliminary stratigraphic and structural architecture of Bhutan: Implications for the along strike architecture of the Himalayan system: Earth and Planetary Science Lett., v. 272 (1-2), pp. 105–117.

Pognante, U. and Benna, P., 1993, Metamorphic zonation, migmatization, and leucogranites along the Everest transect (Eastern Nepal and Tibet): record of an exhumation history. In: Treloar, P. J. and Searle, M. P. (eds.) Himalayan Tectonics. Geol. Soc. London, Spec. Publ. v. 74, pp. 323–340.

Rowley, D. B., 1996, Age of initiation of collision between India and Asia: a review of stratigraphic data. Earth and Planetary Sci. Lett., v. 145, pp. 1-13.

Schelling, D. and Arita, K., 1991, Thrust tectonics, crustal shortening, and the structure of the far-eastern Nepal Himalaya. Tectonics, v. 10 (5), pp. 851-862.

Schelling, D., 1992, The tectonostratigraphy and structure of the eastern Nepal Himalaya. Tectonics, v. 11 (5), pp. 925-943.

Searle, M. P., Law, R. D., Godin, L., Larson, K. P., Streule, M. J., Cottle, J. M., and Jessup, M. J., 2008, Defining the Himalayan Main Central Thrust in Nepal. Jour. Geological Soc., v. 165, pp. 523–534.

Shrestha, S. B., Shrestha, J. N., and Sharma, S. R., 1984, Geological Map of Eastern Nepal, 1:250.000. Ministry of Industry, Department of Mines and Geology, Lainchour, Kathmandu.

Upreti, B. N., 1999, An overview of the stratigraphy and tectonics of the Nepal Himalaya. Jour. Asian Earth Sci., v. 17, pp. 577–606.

Visonà, D. and Lombardo, B., 2002, Two mica- and tormaline leucogranites from the Everest-Makalu region (Nepal-Tibet): Himalayan leucogranite genesis by isobaric heating? Lithos, v. 62, pp. 125–150.

Whitney, D. L., and B. W. Evans, 2010, Abbreviations for names of rock-forming minerals, Am. Mineral., v. 95, pp. 185–187, doi:10.2138/am.2010.3371